Journal of
Materials Chemistry C

PAPER

View Article Online
View Journal | View Issue

Cite this: J. Mater. Chem. C, 2016, 4, 9310

Deep blue-emissive bifunctional (hole-transporting + emissive) materials with $CIE_y \sim 0.06$ based on a 'U'-shaped phenanthrene scaffold for application in organic light-emitting diodes†

Samik Jhulki,[a] Abhaya Kumar Mishra,[a] Avijit Ghosh,[b] Tahsin J. Chow*[b] and Jarugu Narasimha Moorthy*[a]

Received 24th June 2016,
Accepted 7th September 2016

DOI: 10.1039/c6tc02615j

www.rsc.org/MaterialsC

Bifunctional diamines (HTM + EM), namely, **PTPA**, **PDPA** and **PCZL**, have been designed based on a U-shaped phenanthrene scaffold and synthesized in a single step with good isolated yields. In particular, **PTPA** is shown to exhibit deep blue emission ($CIE_{x,y} \sim 0.16, 0.06$) with respectable efficiencies in a simple double layer device.

Introduction

Development of deep blue-emissive materials ($CIE_y < 0.10$) with improved physical as well as electroluminescence properties is of tremendous contemporary interest in organic light-emitting diodes (OLEDs).[1] It is due to the fact that deep blue-emissive materials are more energy efficient than sky blue-emissive materials,[2] and can be utilized as host materials to produce any color by a cascade of energy transfer.[2b] Although highly stable and efficient green-, red- and sky blue-emissive materials have been developed, those that show deep blue emission and exhibit desirable efficiency, stability and color purity are underdeveloped. Consequently, one observes significant focus directed toward developing deep blue-emissive materials based on fluorescence,[1] phosphorescence[1a] and thermally activated delayed fluorescence.[1a] In recent years, several new materials that emit deep blue light have been reported, often with benzimidazole as the emissive fragment, *cf.* Fig. 1.[3] Incidentally, multilayer device fabrication is often a requirement to sequester deep blue emission from these materials.[3] Only a few materials that emit deep blue light when employed in simple double layer devices have been reported.[1,4] Insofar as deep blue emission in double layer devices is concerned, a careful analysis shows that an additional layer of PEDOT:PSS/MoO_3 is invariably present in the fabricated devices.[4–7]

We showed a few years ago that *N*,*N*-diphenylamino-biphenyl-functionalized bimesitylene leads to deep blue emission

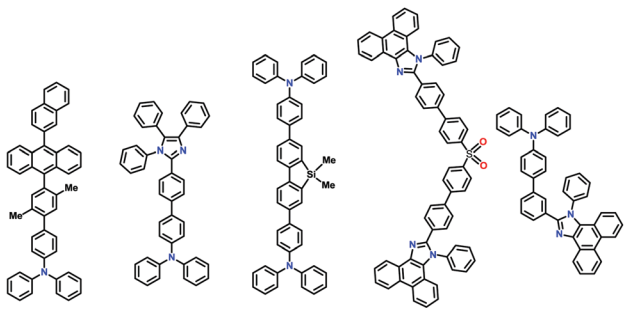

Fig. 1 Structures of some representative deep blue emitters and the results of the device fabrication of these compounds.

with CIE coordinates of (0.15, 0.10) from a true double layer device.[8] However, realization of deep blue-emission with CIEy *ca.* 0.06 from a true double layer device constructed from a bifunctional (hole-transporting + emissive) small molecular organic material is heretofore unknown to the best of our knowledge.[7] To engineer deep blue emission in a double layer device, it is necessary that the material is a bifunctional one. Not surprisingly, such materials are of much commercial demand, as they minimize the production cost by precluding casting of a separate layer.

In continuation of our studies on bifunctional materials based on rigid bimesitylene[8] and Troger's base (TB)[9] as core scaffolds, we reasoned that deep blue-emissive bifunctional materials could be developed based on a U-shaped phenanthrene scaffold functionalized at 3 and 6 positions with suitable secondary aromatic amines, Scheme S1 (ESI†). Our choice of phenanthrene as the scaffold rested on the following considerations: first, the

[a] Department of Chemistry, Indian Institute of Technology, Kanpur 208016, India. E-mail: moorthy@iitk.ac.in; Fax: +91 5122597436; Tel: +91 5122597438
[b] Institute of Chemistry, Academia Sinica, Taipei, Taiwan 115, Republic of China

† Electronic supplementary information (ESI) available: Synthesis details and characterization data, ^1H and ^{13}C NMR spectral reproduction, TGA and DSC profiles, UV-vis, PL and EL plots/profiles. See DOI: 10.1039/c6tc02615j

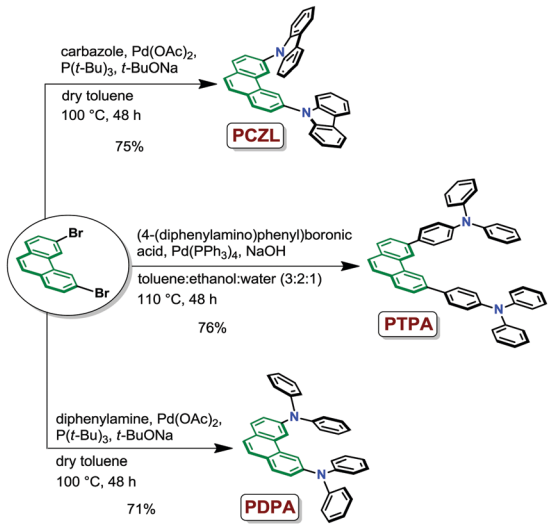

Scheme 1 Synthesis of the target bifunctional diamines.

U-shaped phenanthrene inherently exhibits concave features; compounds that inherently feature concave shapes exhibit packing difficulties, leading to lattice inclusion of guests and amorphous properties.[10] Second, phenanthrene may be considered as an annulated derivative of biphenyl in which the two phenyl rings are stitched together with a double bond at *ortho* positions. Thus, the rigid phenanthrene scaffold can be expected *a priori* to improve the thermal stability, in particular, the T_g. Last, the rigidity and absence of nitrogen atoms (as, for example, in the diazocine moiety of TB) are expected to promote fluorescence properties in the resultant systems, although there exist a large number of compounds in which the amino group is known to enhance fluorescence. Thus, three novel diarylamino derivatives based on phenanthrene, *i.e.*, **PCZL**, **PDPA** and **PTPA**, *cf.* Scheme 1, were synthesized for application as deep-blue emissive bifunctional materials. Herein, we report that these diamines exhibit respectable T_gs and moderate-to-brilliant fluorescence. Sequestration of deep blue emission with a CIEy of ~0.06 is demonstrated for the first time from a simple double layer device fabricated with **PTPA** as a hole-transporting + emissive bifunctional material.

Results and discussion

Synthesis

The synthesis of diamines was accomplished, in respectable isolated yields (71–76%), by employing Suzuki and Buchwald–Hartwig coupling reactions between 3,6-dibromophenanthrene and appropriate boronic acids/secondary aromatic amines, Scheme 1.

Photophysical properties

In Fig. 2a and b UV-vis absorption and fluorescence spectra of the diamines recorded in dilute DCM solutions (*ca.* 1×10^{-5} M) are shown. The UV-vis absorption spectra of the diamines are completely different from each other in terms of spectral features as well as absorption maxima; for example, the longest wavelength maxima for **PCZL**, **PDPA** and **PTPA** lie at 340, 361 and 344 nm, respectively, with different molar absorptivities. Furthermore, the tail-end absorptions for **PDPA** and **PTPA** are bathochromically shifted by *ca.* 50 nm relative to that of **PCZL**, which manifest also in their band gap energies, *vide infra*. Fluorescence spectra show that all compounds emit deep blue fluorescence for excitation at 341 nm. The most blue-shifted and red-shifted emissions are observed for **PCZL** and **PTPA**, which display λ_{max} at 397 and 440 nm, respectively. The order of photoluminescence maxima for **PCZL**, **PDPA** and **PTPA** is consistent with their band gap energies, *cf.* Table 1. In other words, the extent of conjugation is apparently a determining factor in the observed order of photoluminescence maxima. However, in the vacuum sublimed thin films, **PDPA** shows significantly red-shifted (*ca.* 28 nm) emission, although **PCZL** and **PTPA** display emission peaks that are only slightly red and blue shifted, respectively, *cf.* Fig. S1 (ESI†) and Table 1. The change in the order of photoluminescence maxima for **PDPA** and **PTPA** in their thin films must be due to differences in their packings in the solid state, since solvent polarity and its effect in the stabilization of the excited states are no longer operative. A closer analysis of the spectra shows that **PCZL** and **PDPA** display shoulders in their emission spectra, while **PTPA** shows featureless emission, which is due presumably to the differences in the rigidities of their structures. **PCZL** and **PDPA** are more rigid than **PTPA**, which has two additional phenyl spacers in its structure. Fluorescence quantum yields of the compounds determined relative to anthracene as the standard ranged between 16.4 and 79.3% (Table 1).

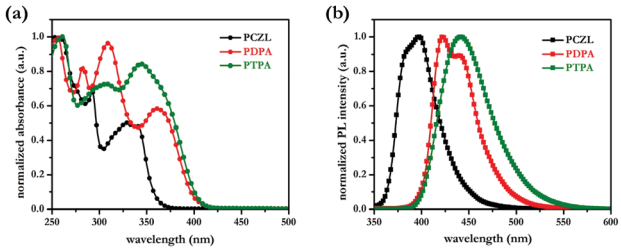

Fig. 2 Normalized absorption (a) and fluorescence (b) spectra (λ_{ex} ~ 341 nm) of **PCZL**, **PDPA** and **PTPA** in DCM.

The higher fluorescence quantum yield of **PCZL** relative to that of **PDPA** is due to the fact that carbazole is a better fluorophore than diphenylamine. As for **PTPA**, its brilliant fluorescence owes origin to two-fold functionalization by triphenylamine groups at 3 and 6 positions of phenanthrene, which leads to the creation of a brilliant fluorophore, namely, diarylaminobiphenyl, in its structure.[8] The possibility of thermally activated delayed fluorescence (TADF) emissions from these compounds can be ruled out based on large differences in their singlet and triplet energies, *cf.* Table 1. The phosphorescence spectra of the phenanthrene compounds are given in Fig. S2 (ESI†).

Electrochemical properties

The CV profiles of all the diamines are given in Fig. S3 (ESI†). While **PCZL** showed irreversible oxidation, the other two diamines, *i.e.*, **PDPA** and **PTPA**, displayed reversible redox behavior.

Table 1 Photophysical, thermal and electrochemical properties of phenanthrene-based materials

Substrate	λ_{max}(UV)[a] (nm)	E_g[b]/E_S[c]/E_T[d] (eV)	λ_{max}(PL)[a] soln/thin film (nm)	Φ_{fl} soln[e] (%)	HOMO[f]/LUMO[g] (eV)	T_g[h]/T_d[i] (°C)
PCZL	292, 329, 340	3.24/3.12/2.55	397/407	16.4	5.24/2.00	129/427
PDPA	283, 309, 361	2.96/2.81/2.38	440/468	13.4	5.11/2.15	93/340
PTPA	307, 344	2.97/2.81/2.33	441/437	79.3	5.27/2.30	111/444

[a] Absorption and fluorescence spectra were recorded in dilute DCM solutions (*ca.* 10^{-5} M). [b] Band gap energies were calculated from red edge absorption onset values using the formula $E = hc/\lambda$. [c] Singlet energies were determined from the fluorescence maxima in DCM. [d] Triplet energies were determined from their 0–0 transitions in the phosphorescence spectra recorded in 2-MeTHF at 77 K. [e] Fluorescence quantum yields were determined for excitation at 341 nm relative to anthracene as the standard. [f] HOMO energies were determined from oxidation potentials in the CV spectra. [g] LUMO energies were calculated by subtracting the band gap energies from HOMO energies. [h] From DSC. [i] From TGA.

HOMO energies of the phenanthrene-diamines were found to range between 5.11 and 5.27 eV, *cf.* Table 1. LUMO energies of the compounds – calculated by subtraction of the band gap energies from HOMO energies – were found to fall in the range of 2.00–2.30 eV. The band gap energies were in turn calculated from tail-end absorption in each case. Thermogravimetric analysis (TGA) revealed high decomposition temperatures (T_ds) for all the diamines in the range of 340–444 °C, *cf.* Fig. S4 (ESI†) and Table 1. Furthermore, they were found to exhibit amorphous properties, as revealed by differential scanning calorimetry (DSC) profiles; the T_gs were found to range between 93 and 129 °C, *cf.* Fig. S5 (ESI†) and Table 1. Indeed, T_gs of the diamines are comparable to or better than those of the commercially available HTMs such as NPB[11a] and TPD.[11b]

Electroluminescence properties

To begin with, the emissive properties of phenanthrene diamines were examined by fabricating devices with the following configuration: (A) ITO/NPB (40 nm)/**PCZL** or **PDPA** or **PTPA** (10 nm)/TPBI (40 nm)/LiF (1 nm)/Al (150 nm), where ITO functions as the anode, NPB serves as a hole-transporting material, 2,2′,2″-(1,3,5-benzinetriyl)tris(1-phenyl-1*H*-benzimidazole) (TPBI) serves as an electron-transporting as well as hole-blocking material and LiF/Al as the composite cathode; of course, the emissive layer was cast with phenanthrene-based emitters in each case. The electroluminescence spectra and *I*–*V*–*L* plots recorded for the devices thus constructed are shown in Fig. S6 and S7 (ESI†), respectively. The device performance results are collected in Table 2.

As can be perused from the data in Table 2, all phenanthrene diamines function as emissive materials in simple OLED devices with low turn-on voltages and moderate external quantum efficiencies. Insofar as the EL spectra in device configuration A are concerned (Fig. S7, ESI†), both **PCZL** and **PDPA** show pure emission, while **PTPA** displays an additional peak at *ca.* 490 nm due to exciplex formation with the overall emission corresponding to sky blue color with the CIE coordinates of (0.19, 0.23). To sequester deep blue emission by eliminating the exciplex emission, a slightly modified device of the following configuration with variation in the layer thicknesses was fabricated: (B) ITO/NPB (40 nm)/**PTPA** (20 nm)/TPBI (35 nm)/LiF (1 nm)/Al (150 nm). Indeed, it was found that the peak at a longer wavelength observed for device A completely disappeared for device B with the emission from **PTPA** corresponding to deep blue (CIE ∼ 0.17, 0.08), *cf.* Fig. S7 (ESI†); the latter is very close to those of NTSC standard blue (CIE ∼ 0.14, 0.08).

The phenanthrene diamines **PCZL**, **PDPA** and **PTPA** are essentially high HOMO (5.11–5.27 eV) systems that display respectable fluorescence. It was thus expected that they could also serve the dual role of hole transport as well as emission in simple double layer devices. To probe the same, double layer devices of the following configuration were fabricated: (C) ITO/**PTPA** or **PCZL** or **PDPA** (60 nm)/TPBI (40 nm)/LiF (1 nm)/Al (150 nm). The results of electroluminescence from these devices are collected in Table 2. The *I*–*V*–*L* and EL plots are given in Fig. S9 (ESI†) and Fig. 3, respectively.

A perusal of the data in Table 2 reveals that the device performance results with **PTPA** as a bifunctional material are

Table 2 Application of **PCZL**, **PDPA** and **PTPA** as EMs and HTMs

Substrate	Device[a]	V_{on}[b]	η_{ex}[c]	η_p[d]	η_l[e]	L_{max}[f]	CIE[g] (x, y)	fwhm[h]
PTPA	A	3.0	1.51	2.49	2.70	5960	0.19, 0.23	118
	B	3.0	1.98	1.00	1.12	1590	0.17, 0.08	48
	C	3.5	1.97	0.88	0.98	1890	0.16, 0.06	44
PCZL	A	3.5	1.50	1.01	1.19	3100	0.16, 0.11	64
	C	8.5	0.55	0.12	0.36	534	0.16, 0.08	60
	D	6.0	2.39	0.81	1.81	889	0.16, 0.08	52
PDPA	A	3.0	0.67	0.81	0.87	2550	0.17, 0.16	100
	C	3.5	1.18	0.79	1.26	1720	0.16, 0.13	76
	D	3.5	2.40	1.51	1.68	1270	0.17, 0.08	52

[a] A–D refer to the device configurations, see the text. [b] Turn-on voltage (V). [c] Maximum external quantum efficiency (%). [d] Maximum power efficiency (lm W^{-1}). [e] Maximum luminous efficiency (cd A^{-1}). [f] Maximum luminance achieved (cd m^{-2}). [g] 1931 chromaticity coordinates measured at 6 V. [h] Full width at half maximum (nm).

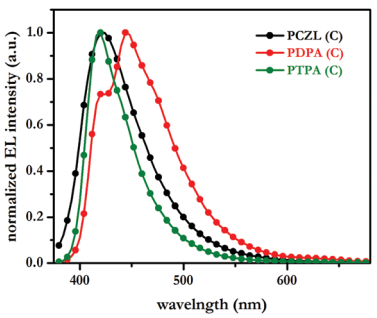

Fig. 3 EL spectra of devices C in which **PCZL**, **PDPA** and **PTPA** serve as bifunctional materials; note the narrow distribution of the EL spectrum of **PTPA**.

far better than those obtained with the other two materials, *i.e.*, **PDPA** and **PCZL**. The most attractive feature is the narrow EL of **PTPA** with a full width at half maximum (fwhm) of only 44 nm; this value is indeed amongst the lowest values reported for bifunctional materials.[3] The corresponding CIE coordinates are (0.16, 0.06) at 6 V. The occurrence of such highly pure deep blue color is rare, and rarer are those that exhibit such deep blue emission in double layer devices.[3–8] The maximum external quantum efficiency and luminance for the devices of **PTPA** are 1.97% and 1890 cd m^{-2}. For comparison, note that a structurally similar unipolar material, *i.e.*, a two-fold triarylamino-functionalized 5,5-dimethyl-5*H*-dibenzo[*b*,*d*]silole (Fig. 1), displays an external quantum efficiency of only 1.19% in a three-layer device; the latter is much lower than that obtained from the **PTPA**-based double layer device. It is, however, true that deep blue emissions with better efficiencies have been captured from many other materials, but the requirement of multilayer device fabrication is a drawback with these materials.[3] Moreover, many such materials have bipolar architectures;[3b,f] the introduction of bifunctionality necessitates a multistep synthesis. In contrast, **PTPA** is a unipolar material that can be accessed in a single step with very good isolated yield, and is therefore a value addition to the family of bifunctional HTMs. A disadvantage with unipolar materials such as **PTPA**, however, is that the disparity in the supply of holes and electrons to the emissive zone leads to reduction in the efficiency; the latter is further worsened by the fact that the holes migrate several orders of magnitude faster than electrons. It is thus not surprising that the efficiencies obtained from **PTPA** do not compare with those of the other bipolar materials that exhibit deep blue emission. Notwithstanding the relatively lesser efficiency, the fact that the deep blue light with CIEy $\sim$ 0.06 is sequestered from a simple double layer device with a bifunctional and unipolar **PTPA** is indeed remarkable.

Spurred by the excellent device performance results obtained with **PTPA** in device C, similar devices were also fabricated for **PCZL** and **PDPA**. The device performance results with **PDPA** as a hole-transporting as well as emissive material are moderate. **PCZL** performs more poorly under similar conditions, *cf.* Table 2. The reason for better results with **PTPA** is primarily a consequence of its higher fluorescence quantum yield when compared to those of **PCZL** and **PDPA**. The slightly lower LUMO level of **PTPA** relative to those of the other two facilitates electron injection from the electron transport layer, which may also contribute to the observed high efficiency for **PTPA**. Nonetheless, both **PCZL** and **PDPA** emit deep blue light with CIE coordinates of (0.16, 0.08) and (0.16, 0.13), respectively, when employed in double layer devices. To further emphasize the hole-transporting abilities of **PCZL** and **PDPA**, device D of the following configuration was also fabricated: (D) ITO/**PCZL** or **PDPA** (40 nm)/**PTPA** (20 nm)/TPBI (35 nm)/LiF (1 nm)/Al (150 nm), wherein both HTM (**PCZL**/**PDPA**) and EM (**PTPA**) are based on the phenanthrene scaffold. *I–V–L* characteristics of all devices and EL spectra of device C are shown in Fig. S9 (ESI†) and Fig. 3, respectively. Relevant efficiency plots are given in the ESI.† The device performance results collected in Table 2 suggest that both **PCZL** and **PDPA** serve as HTMs, indeed better than the standard NPB insofar as maximum efficiencies are concerned. We attribute this slightly better performance of **PCZL** and **PDPA** as HTMs – relative to NPB – to the structural compatibility between phenanthrene-based materials. Note that maximum EQE values in device D are higher than those obtained from device B, although maximum luminances show the opposite trend. This is not surprising as the rate of efficiency roll-off is higher in device D when compared to that in B. Indeed, device B shows higher efficiency than device D at high luminance values. Furthermore, EL spectra captured from devices B and D are similar, as the emissive species is the same, *i.e.*, **PTPA**. A comparison of the EL spectrum of **PTPA** with its PL spectrum shows that the former is blue-shifted, which may arise due to microcavity effects.[3a,b]

As mentioned at the outset, NPB and TPD have found extensive application as HTMs, despite their noted drawback with low T_g.[1] Although the latter has been circumvented in many novel HTMs, search for compounds that entail simple synthesis and show respectable T_gs continues unabated. In this context, the materials that show dual properties, *i.e.*, hole transport as well as emission, are particularly important. From our systematic investigations, it is shown that phenanthrene-based materials are HTMs, and that they also serve the purpose of emission in simple double layer devices. **PTPA** is not only better than the other two materials, *i.e.*, **PCZL** and **PDPA**, investigated in the present investigation, but also than several other reported materials that exhibit a dual role.[1]

Conclusions

In conclusion, three novel electroluminescent materials, *i.e.*, **PCZL**, **PDPA** and **PTPA**, were designed based on a U-shaped phenanthrene scaffold and synthesized readily starting from 3,6-dibromophenanthrene by Buchwald–Hartwig and Suzuki coupling protocols. These molecular materials display high T_ds, respectable T_gs and moderate-to-high fluorescence. In simple nondoped devices, the diamines are demonstrated to function as emissive materials. Furthermore, in double layer devices, they are shown to function as bifunctional, *i.e.*, hole-transporting as well as emissive materials. In particular, **PTPA** is shown to emit deep blue light with CIE coordinates of (0.16, 0.06), and respectable luminance and external quantum efficiency of 1890 cd m^{-2} and 1.97%, respectively. The results constitute the first demonstration of deep blue emission with CIEy $\sim$ 0.06 from a simple double layer device constructed from a bifunctional (hole-transporting + emissive) diamine, *i.e.* **PTPA**. The CIE coordinates match the quality demanded by HDTV and European Broadcasting Union standard. The moderate efficiency with respectable luminance in conjunction with high color purity, low CIE coordinates and easy synthesis makes **PTPA** a standout addition to the ever-expanding library of HTMs.

Experimental section

Characterization of physical properties and device fabrication

Characterization of thermal and photophysical properties and device fabrication were carried out as described elsewhere.[9,12]

Typically, the patterned ITO-coated glass slides were cleaned sequentially in a detergent solution, distilled water (4 times), isopropanol and acetone by rigorous ultrasonication for 15 min in each medium. After drying in a flow of nitrogen, the glass slides were further subjected to three cycles of oxygen plasma treatment (All Real Tech. PCD150) at 40–45 W for 5 min to remove trace amounts of impurities. Later, the glass slides were transferred to a vacuum chamber maintained at a very low pressure (10^{-5} to 10^{-6} Torr), and placed in a rotating holder firmly. Materials kept in crucibles were heated sequentially, as per the device configuration, to cause deposition onto the ITO-coated glass slides. The deposition rate was 0.4–1.0 Å s^{-1}. A quartz thickness controller placed near the rotating disk guided the thickness of each layer. After completion of evaporation without breaking the vacuum, the devices were taken out from the sublimation chamber and kept in a glove box maintained at a very low pressure of oxygen and moisture. Finally, the devices were sealed by cover glasses containing UV-cured epoxy glue at the periphery. The *I–V–L* characteristics and other measurements of the fabricated devices were performed under ambient conditions without any precaution using a Keithly 2400 source meter connected to a PR650 spectrophotometer.

Synthesis of 3,6-dibromophenanthrene

This compound was prepared by following the literature-reported procedure.[13] ^{1}H NMR ($CDCl_3$, 400 MHz) δ 7.70–7.77 (m, 6H), 8.72 (d, J = 1.96 Hz, 2H).

Synthesis of PCZL

An oven-dried pressure tube containing 10 mL of dry toluene was degassed thoroughly by bubbling N_2 gas for 10 min. To this were added 3,6-dibromophenanthrene (0.30 g, 0.89 mmol), carbazole (0.26 g, 1.96 mmol), sodium *tert*-butoxide (0.40 g, 3.57 mmol), P(^{t}Bu)$_3$ (22 μL, 0.09 mmol) and $Pd(OAc)_2$ (0.02 g, 0.09 mmol). Subsequently, the pressure tube was capped tightly under nitrogen and the contents of the mixture were heated at 100 °C for 48 h. At the end of this period, the pressure tube was cooled to rt and the toluene was removed *in vacuo*. The crude reaction mixture was extracted three times with chloroform, and the combined organic extract was dried over anhyd Na_2SO_4. Evaporation of the organic solvent led to the crude product, which was purified by silica gel column chromatography to afford **PCZL** as a colorless solid, yield 0.34 g (75%); mp 291 °C; IR (KBr) cm^{-1} 3054, 1601, 1514, 1449, 1359, 1334; ^{1}H NMR ($CDCl_3$, 400 MHz) δ 7.30 (td, J_1 = 7.34 Hz, J_2 = 0.92 Hz, 4H), 7.40 (td, J_1 = 7.06 Hz, J_2 = 0.92 Hz, 4H), 7.49 (d, J = 8.24 Hz, 4H), 7.87 (dd, J_1 = 8.50 Hz, J_2 = 2.06 Hz, 2H), 7.97 (s, 2H), 8.16 (d, J = 7.80 Hz, 4H), 8.19 (d, J = 8.72 Hz, 2H), 8.80 (d, J = 1.84 Hz, 2H); ^{13}C NMR ($CDCl_3$, 125 MHz) δ 109.6, 120.2, 120.4, 121.0, 123.5, 126.1, 126.3, 127.0, 130.5, 131.1, 131.2, 136.4, 141.0; EI-MS$^+$ m/z [M]$^+$ calcd for $C_{38}H_{24}N_2$ 508.1939, found 508.1938.

Synthesis of PDPA

A similar procedure to that described above for the synthesis of **PCZL** was followed for the synthesis of **PDPA** as well. The reaction between 3,6-dibromophenanthrene (0.30 g, 0.89 mmol) and diphenylamine (0.26 g, 1.96 mmol) in the presence of sodium *tert*-butoxide (0.40 g, 3.57 mmol), P(^{t}Bu)$_3$ (22 μL, 0.09 mmol) and $Pd(OAc)_2$ (0.02 g, 0.09 mmol), followed by work up and column chromatography afforded **PDPA** as a yellowish-green solid material, yield 0.33 g (71%); mp 243 °C; IR (KBr) cm^{-1} 3033, 1589, 1490, 1436, 1314; ^{1}H NMR ($CDCl_3$, 500 MHz) δ 7.03 (t, J = 7.15 Hz, 4H), 7.10 (d, J = 7.45 Hz, 8H), 7.22 (t, J = 7.72 Hz, 8H), 7.32 (dd, J_1 = 8.60 Hz, J_2 = 1.15 Hz, 2H), 7.54 (s, 2H), 7.71 (d, J = 8.60 Hz, 2H), 7.89 (s, 2H); ^{13}C NMR ($CDCl_3$, 125 MHz) δ 116.3, 122.9, 123.9, 124.3, 124.9, 128.1, 129.2, 129.3, 130.7, 146.1, 147.6; EI-MS$^+$ m/z [M]$^+$ calcd for $C_{38}H_{28}N_2$ 512.2252, found 512.2254.

Synthesis of PTPA

To an oven-dried pressure tube were added 12 mL of toluene, 8 mL of ethanol and 4 mL of distilled water. The resultant mixture was degassed thoroughly by bubbling N_2 gas for 10 min. Subsequently, 3,6-dibromophenanthrene (0.50 g, 1.48 mmol), (4-(diphenylamino)-phenyl)boronic acid (1.72 g, 5.95 mmol), NaOH (0.36 g, 8.88 mmol) and $Pd(PPh_3)_4$ (0.34 g, 0.30 mmol) were introduced and the pressure tube was capped tightly under N_2 gas. The contents of the mixture were heated at 110 °C for 48 h. At the end of the period, the pressure tube was cooled to rt, and toluene and ethanol were removed *in vacuo*. The residue was extracted three times with chloroform and the combined organic extracts were dried over anhyd Na_2SO_4. Evaporation of the organic solvents led to the crude product, which was subjected to silica gel column chromatography to afford **PTPA** as a colorless solid, yield 0.75 g (76%); mp 218 °C; IR (KBr) cm^{-1} 3031, 2921, 1590, 1492, 1436, 1314; ^{1}H NMR ($CDCl_3$, 400 MHz) δ 7.06 (t, J = 7.32 Hz, 4H), 7.18 (dd, J_1 = 7.32 Hz, J_2 = 1.40 Hz, 8H), 7.23 (d, J = 8.68 Hz, 4H), 7.28–7.32 (m, 8H), 7.68 (d, J = 8.72 Hz, 4H), 7.75 (s, 2H), 7.83 (dd, J_1 = 6.88 Hz, J_2 = 1.40 Hz, 2H), 7.95 (d, J = 8.28 Hz, 2H), 8.91 (d, J = 1.40 Hz, 2H); ^{13}C NMR ($CDCl_3$, 125 MHz) δ 120.4, 123.0, 124.0, 124.5, 125.8, 126.4, 128.3, 129.1, 129.3, 130.6, 131.2, 135.3, 138.9, 147.4, 147.7; ESI-MS$^+$ m/z [M]$^+$ calcd for $C_{50}H_{36}N_2$ 664.2878, found 664.2870.

Acknowledgements

JNM is thankful to SERB, India, for generous financial support. SJ and AKM gratefully acknowledge Senior Research Fellowships from CSIR and UGC, respectively. We thankfully acknowledge the support from the Scientific Instruments Facility at the Institute of Chemistry, Academia Sinica, for optoelectronic device fabrication and testing.

Notes and references

1 (*a*) X. Yang, X. Xu and G. Zhou, *J. Mater. Chem. C*, 2015, **3**, 913; (*b*) W.-C. Chen, C.-S. Lee and Q. X. Tong, *J. Mater. Chem. C*, 2015, **3**, 10957; (*c*) S. Kim, B. Kim, J. Lee, H. Shin, Y. Park and J. Park, *Mater. Sci. Eng., R*, 2016, **99**, 1; (*d*) K. Müllen and U. Scherf, *Organic Light Emitting Devices: Synthesis, Properties and Applications*, Wiley-VCH Verlag GmbH & Co. KGaA, Weinheim, 2006.

2 (*a*) S. Chen, L. Deng, J. Xie, L. Peng, L. Xie, Q. Fan and W. Huang, *Adv. Mater.*, 2010, **22**, 5227; (*b*) C. Liu, Y. Li, C. Yang, H. Wu, J. Qin and Y. Cao, *Chem. Mater.*, 2013, **25**, 3320.

3 (*a*) R. Kim, S. Lee, K.-H. Kim, Y.-J. Lee, S.-K. Kwon, J.-J. Kim and Y.-H. Kim, *Chem. Commun.*, 2013, **49**, 4664; (*b*) W. Li, L. Yao, H. Liu, Z. Wang, S. Zhang, R. Xiao, H. Zhang, P. Lu, B. Yang and Y. Ma, *J. Mater. Chem. C*, 2014, **2**, 4733; (*c*) X.-K. Liu, C.-J. Zheng, M.-F. Lo, J. Xiao, C.-S. Lee, M.-K. Fung and X.-H. Zhang, *Chem. Commun.*, 2014, **50**, 2027; (*d*) S. F. Chen, Y. Tian, J. Peng, H. Zhang, X. J. Feng, H. Zhang, X. Xu, L. Li and J. Gao, *J. Mater. Chem. C*, 2015, **3**, 6822; (*e*) X. Tang, Q. Bai, Q. Peng, Y. Gao, J. Li, Y. Liu, L. Yao, P. Lu, B. Yang and Y. Ma, *Chem. Mater.*, 2015, **27**, 7050; (*f*) H. Liu, Q. Bai, L. Yao, H. Zhang, H. Xu, S. Zhang, W. Li, Y. Gao, J. Li, P. Lu, H. Wang, B. Yang and Y. Ma, *Chem. Sci.*, 2015, **6**, 3797; (*g*) Y.-H. Chung, L. Sheng, X. Xing, L. Zheng, M. Bian, Z. Chen, L. Xiao and Q. Gong, *J. Mater. Chem. C*, 2015, **3**, 1794.

4 (*a*) C. Liu, Y. Li, Y. Zhang, C. Yang, H. Wu, J. Qin and Y. Cao, *Chem. – Eur. J.*, 2012, **18**, 6928; (*b*) S. Xue, X. Qiu, L. Yao, L. Wang, M. Yao, C. Gu, Y. Wang, Z. Xie and H. Wu, *Org. Electron.*, 2015, **27**, 35; (*c*) M. Yu, S. Wang, S. Shao, J. Ding, L. Wang, X. Jing and F. Wang, *J. Mater. Chem. C*, 2015, **3**, 861; (*d*) H. Xiao, L. Ding, D. Ruan, B. Li, N. Ding and D. Ma, *Dyes Pigm.*, 2015, **121**, 7.

5 For deep blue emission from an oligomeric material in a *true* double layer device, see: Z. H. Li, M. S. Wong, Y. Tao and J. Lu, *Chem. – Eur. J.*, 2005, **11**, 3285.

6 For deep blue emission from a polymeric material in a *true* double layer device, see: C. W. Huang, C. L. Tsai, C. Y. Liu, T. H. Jen, N. J. Yang and S. A. Chen, *Macromolecules*, 2012, **45**, 1281.

7 A bifunctional material that is electron-transporting and emissive has been employed in a true double layer device to sequester deep blue emission with CIEy $\sim$ 0.07, see: C. H. Chien, C. K. Chen, F. M. Hsu, C. F. Shu, P. T. Chou and C. H. Lai, *Adv. Funct. Mater.*, 2009, **19**, 560.

8 J. N. Moorthy, P. Venkatakrishnan, D.-F. Huang and T. J. Chow, *Chem. Commun.*, 2008, 2146.

9 (*a*) I. Neogi, S. Jhulki, M. Rawat, R. S. Anand, T. J. Chow and J. N. Moorthy, *RSC Adv.*, 2015, **5**, 26806; (*b*) I. Neogi, S. Jhulki, A. Ghosh, T. J. Chow and J. N. Moorthy, *Org. Electron.*, 2014, **15**, 3766.

10 Concave features often promote guest inclusion behaviour, see: (*a*) E. M. Veen, P. M. Postma, H. T. Jonkman, A. L. Spek and B. L. Feringa, *Chem. Commun.*, 1999, 1709; (*b*) I. Neogi, A. Bajpai, G. Savitha and J. N. Moorthy, *Cryst. Growth Des.*, 2015, **15**, 2129, and references therein.

11 (*a*) S. A. Van Slyke, C. H. Chen and C. W. Tang, *Appl. Phys. Lett.*, 1996, **69**, 2160; (*b*) K. Naito and A. Miura, *J. Phys. Chem.*, 1993, **97**, 6240.

12 I. Neogi, S. Jhulki, A. Ghosh, T. J. Chow and J. N. Moorthy, *ACS Appl. Mater. Interfaces*, 2015, **7**, 3298.

13 H. R. Talele, A. R. Chaudhary, P. R. Patel and A. V. Bedekar, *ARKIVOC*, 2011, 15.